EC
Journals.ASM.org

Three Prevacuolar Compartment Rab GTPases Impact *Candida albicans* Hyphal Growth

Douglas A. Johnston, Arturo Luna Tapia, Karen E. Eberle, Glen E. Palmer

Department of Microbiology, Immunology, and Parasitology, Louisiana State University Health Sciences Center, School of Medicine, New Orleans, Louisiana, USA

Disruption of vacuolar biogenesis in the pathogenic yeast *Candida albicans* causes profound defects in polarized hyphal growth. However, the precise vacuolar pathways involved in yeast-hypha differentiation have not been determined. Previously we focused on Vps21p, a Rab GTPase involved in directing vacuolar trafficking through the late endosomal prevacuolar compartment (PVC). Herein, we identify two additional Vps21p-related GTPases, Ypt52p and Ypt53p, that colocalize with Vps21p and can suppress the hyphal defects of the *vps21*Δ/Δ mutant. Phenotypic analysis of gene deletion strains revealed that loss of both *VPS21* and *YPT52* causes synthetic defects in endocytic trafficking to the vacuole, as well as delivery of the virulence-associated vacuolar membrane protein Mlt1p from the Golgi compartment. Transcription of all three GTPase-encoding genes is increased under hyphal growth conditions, and overexpression of the transcription factor Ume6p is sufficient to increase the transcription of these genes. While only the *vps21*Δ/Δ single mutant has hyphal growth defects, these were greatly exacerbated in a *vps21*Δ/Δ *ypt52*Δ/Δ double mutant. On the basis of relative expression levels and phenotypic analysis of gene deletion strains, Vps21p is the most important of the three GTPases, followed by Ypt52p, while Ypt53p has an only marginal impact on *C. albicans* physiology. Finally, disruption of a nonendosomal AP-3-dependent vacuolar trafficking pathway in the *vps21*Δ/Δ *ypt52*Δ/Δ mutant, further exacerbated the stress and hyphal growth defects. These findings underscore the importance of membrane trafficking through the PVC in sustaining the invasive hyphal growth form of *C. albicans*.

The fungal vacuole plays a vital role in supporting the pathogenicity of *Candida albicans* and *Cryptococcus neoformans* (1–3) and is likely to be critical for other fungal pathogens to cause disease (4, 5). In both *C. albicans* and *C. neoformans*, defects in vacuolar function result in a number of pathogenesis-related phenotypes, including susceptibility to host-related stresses and loss of virulence-related attributes (1, 2, 6–8). Vacuole-deficient *C. albicans* mutants have profound defects in invasive hyphal growth (3, 6, 9), which is crucial for virulence (10, 11).

Gow and Gooday first observed that the fungal vacuole expands dramatically during *C. albicans* hyphal growth to yield extensively vacuolated subapical compartments (12). While several subsequent studies have established that vacuolar biogenesis plays a crucial role in supporting polarized hyphal growth, the contribution of individual trafficking pathways is unknown. Multiple vacuolar trafficking pathways have been identified in the model yeast *Saccharomyces cerevisiae* (13). Several vacuolar proteins, including carboxypeptidase Y, are delivered to the vacuole through a major biosynthetic trafficking route from the Golgi apparatus via the late endosome (also known as the prevacuole compartment [PVC]). This endosomal route is dependent upon the Rab GTPase Vps21p (14–16). A second Golgi-to-vacuole pathway sorts cargo, including alkaline phosphatase (ALP), into a distinct set of vesicles that bypass the late endosome and are delivered directly to the vacuole. The ALP trafficking pathway is facilitated by the AP-3 coat complex, which has four subunits, including Aps3p (17, 18). Endocytosis delivers cell surface proteins to the vacuole for degradation, also occurs via the PVC compartment, and is also dependent upon Vps21p (15, 19–22). Our previous study revealed that loss of both Vps21p-dependent (endosomal) and Aps3p-dependent (nonendosomal) vacuolar pathways renders *C. albicans* severely impaired in the capacity to form hyphae (3). Despite these defects, the *vps21*Δ/Δ*aps3*Δ/Δ double mutant maintained a largely intact vacuole morphology in the yeast form and most of a vacuolar membrane marker protein (Mlt1-green fluorescent protein [GFP]) reached its destination. This indicated that additional Golgi-to-vacuole trafficking routes must exist in *C. albicans*. The purpose of this study was to define these pathways and determine their role in *C. albicans* hyphal growth.

MATERIALS AND METHODS

Growth conditions. Strains were routinely grown on yeast extract-peptone-dextrose (YPD) at 30°C and supplemented with uridine (50 μg ml^{-1}) when necessary. For growth curve determination, overnight cultures were subcultured into 20 ml fresh YPD medium to an optical density at 600 nm (OD_{600}) of 0.2 and incubated at 30°C with shaking. OD_{600} was determined from samples taken hourly. Transformants were selected on minimal medium (6.75 g $liter^{-1}$ yeast nitrogen base plus ammonium sulfate and without amino acids, 2% dextrose, 2% Bacto agar; YNB) supplemented with the appropriate auxotrophic requirements as described for *S. cerevisiae* (23) or uridine at 50 μg ml^{-1}.

Plasmid construction. Plasmids pGEMURA3, pGEMHIS1, pRSARGΔSpe, and pDDB57 (24, 25) were provided by A. Mitchell (Carnegie Mellon University), pLUX (26) was provided by W. Fonzi (Georgetown University), pCaDis (27) was provided by P Sudbery (University of Sheffield), and pCAU97 was provided by H. Nakayama and M. Arisawa (Nippon Roche). Plasmids pLUXVPS21, pLUXGFP-VPS21, and pLUXAPS3 were previously constructed (3, 6). Plasmids pLUXYPT52 and pLUXYPT53 were made as follows. The *YPT52* or *YPT53* open read-

Received 20 December 2012 Accepted 20 May 2013
Published ahead of print 24 May 2013
Address correspondence to Glen E. Palmer, gpalme@lsuhsc.edu.
D.A.J. and A.L.T. contributed equally to this work.
Supplemental material for this article may be found at http://dx.doi.org/10.1128/EC.00359-12.

doi:10.1128/EC.00359-12

ing frame (ORF) with 5′ and 3′ untranslated region (UTR) sequences was amplified from SC5314 genomic DNA (gDNA) with HiFi Platinum *Taq* (Invitrogen) and primer set YPT52AMPF2-YPT52AMPR or YPT53AMPF-YPT53AMPR (see Table S1 in the supplemental material). The purified *YPT52* product was then cloned between the KpnI and SacI sites of the vector pLUX, and *YPT53* was cloned into the BamHI site of pLUX. Plasmid pKE1 was constructed as follows. One kilobase of the *ACT1* promoter (*ACT1p*) sequence was amplified from gDNA (strain SC5314 [28]) with primers ACT1PF and ACT1PR2 and platinum HiFi *Taq* polymerase (Invitrogen) and cloned between the KpnI and SacI sites of pLUX. The 3′ UTR sequences of the *ADH1* gene were then amplified from SC5314 gDNA with primers ADH1-3′UTRF and ADH1-3′UTRR and cloned downstream of *ACT1p* between the SalI and SacI restriction sites, incorporating a multiple cloning site between the *ACT1p* and *ADH1* 3′ UTR sequences consisting of SalI, ClaI, EagI, MluI, and SphI sites. pACT1-YPT53 was made by amplifying the *YPT53* ORF with primers YPT53ORFF-CLAI and YPT53ORFR-MLUI and cloning the product between the ClaI and MluI sites of pKE1.

To produce GFP and mCherry fusion proteins, the ATG start codon of *YPT52* in pLUXYPT52 or *YPT53* in pLUXYPT53 was replaced with an EagI site by site-directed mutagenesis with the QuikChange kit (Stratagene) and primer set YPT52EAGF/R or YPT53EAGF/R. *C. albicans* optimized GFP or mCherry coding sequences were amplified from pGFPURA3 (29) or pMG2254 (30) with primer set GFPEAGF/R or MCHORFF/R and cloned into the EagI site of the modified pLUXYPT52 or pLUXYPT53 plasmid. Correct orientation and in-frame fusions were confirmed by sequencing the respective clones with primer GFPSEQF (GFP fusions) or with YPT52DETR or YPT53DETR (mCherry fusions). GFP-*VPS21* was amplified from pLUXGFPVPS21 with primers GFPSALIF–VPS21ORFR-MLUI and cloned between the SalI and MluI sites of pKE1 to yield the *ACT1*-GFP-*VPS21* construct. Each of the mCherry fusions was also amplified with MCHORFF–YPT52ORFR-MLUI or YPT53ORFR-MLUI and cloned between the SalI and MluI sites of pKE1. Finally, the *ACT1p*-mCherry-*YPT52-ADH3′*UTR and *ACT1p*-mCherry-*YPT52-ADH3′*UTR cassettes were amplified from the above-described pKE1-derived clones with primers ACT1PF-BAMHI and ADH13′UTRR-APAI and cloned between the BamHI and ApaI sites of pGEMHIS1. pAPS3tr was made by PCR amplifying a 281-nucleotide (nt) portion of ORF *APS3* lacking the first 51 nt and the last 129 nt of the coding sequence with primers APS3FRAGF and APS3FRAGR2. This *APS3* fragment falls within the portion of *APS3* deleted as outlined below. The purified PCR product was cloned between the SalI and MluI sites of pGEMURA3.

Plasmid pKEtetO4 was constructed by amplifying the *tetO* promoter from plasmid pCAU97 (31) with primers TETOAMPF/R and cloning the product between the KpnI and SalI sites of pKE1 in place of *ACT1p*. *UME6* was then amplified with primers UME6ORFF-SalI and UME6ORFR-MluI and cloned downstream of the *tetO* promoter between the SalI and MluI sites of pKEtetO4 to make pKEtetO4-UME6.

Site-directed mutagenesis. Active and inactive conformational *YPT72*, *VPS21*, *YPT52*, and *YPT53* mutants were generated with the QuikChange kit (Stratagene) and primer sets YPT72T24NF/R, YPT72Q70LF/R, VPS21S24NF/R, VPS21Q69LF/R, YPT52S26NF/R, YPT52Q73LF/R, YPT53T27NF/R, and YPT53Q75LF/R, respectively.

Strain construction. Gene deletion strains were constructed by the PCR-based approach described by Wilson et al., with *ura3*$^-$ *his1*$^-$ *arg4*$^-$ mutant strain BWP17 (24), which was kindly provided by A. Mitchell (Carnegie Mellon University). *C. albicans* was transformed by the lithium acetate procedure (32). The *vps21*Δ/Δ, *ypt72*Δ/Δ, and *aps3*Δ/Δ mutants were constructed in previous studies (3, 6). Gene deletion cassettes were amplified with primer set YPT52DISF-YPT52DISR, YPT53DISF-YPT53DISR, or APS3DISF-APS3DISR with pARGΔSpe (*ARG4* marker), pGEMHIS1 (*HIS1* marker), or pDDB57 (recyclable *URA3-dpl200* cassette) as the template. To make *ypt52*Δ/Δ and *ypt53*Δ/Δ single-gene deletion strains, alleles were sequentially replaced with *HIS1* and *ARG4* selection markers.

The *vps21*Δ/Δ *ypt52*Δ/Δ and *vps21*Δ/Δ *ypt53*Δ/Δ double mutants were made from a *vps21*Δ/Δ*ura3*$^-$ *arg4*$^-$ strain previously constructed (6), by sequentially deleting both the *YPT52* and *YPT53* alleles with first the recyclable *URA3-dpl200* selection marker and then the *ARG4* marker. The regeneration of *ura3*$^-$ recombinants was then selected on YNB medium supplemented with uridine and 1 μg ml^{-1} 5-fluoroorotic acid (5-FOA) (33). The *ypt52*Δ/Δ *ypt53*Δ/Δ double mutant was made by a similar approach necessitating two rounds of 5-FOA selection to recycle the *URA3* selection marker. The correct integration of either gene deletion cassette was confirmed at each step by diagnostic PCR with primers ARG4DET2-YPT52AMPR, -YPT53AMPR, or -APS3AMPR (*ARG4* integration); HIS1F1268-YPT52AMPF, -YPT53AMPF, or -APS3AMPF (*HIS1* integration); or URAINTF-YPT52AMPR, -YPT53AMPR, or -APS3AMPR and URAINTR-YPT52AMPF, -YPT53AMPF, or -APS3AMPF (*URA3* integration). The absence of either the *YPT52* or the *YPT53* ORF following the deletion of both alleles was confirmed by PCR with primer pair YPT52DETF-YPT52AMPR or YPT53DETF-YPT53AMPR, respectively.

The 5-FOA-selected *ura3*$^-$ *vps21*Δ/Δ *ypt52*Δ/Δ mutant strain was transformed with a *ypt53*Δ:*URA3-dpl200* cassette to delete one copy of *YPT53*. Following a further round of 5-FOA selection, the *ura3*$^-$ *vps21*Δ/Δ *ypt52*Δ/Δ *ypt53*Δ/*YPT53* mutant strain was transformed with NheI-cut pLUXYPT53^{T27N} containing a dominant negative *YPT53* allele. Finally, the *ura3*$^-$ *vps21*Δ/Δ *ypt52*Δ/Δ mutant strain was transformed with an *aps3*Δ:*URA3-dpl200* cassette to delete one copy of *APS3*. Following a further round of 5-FOA selection, the second *APS3* allele was targeted by insertional inactivation; the *ura3*$^-$ *vps21*Δ/Δ *ypt52*Δ/Δ*aps3*Δ/*APS3* mutant strain was transformed with pAPS3tr, which was linearized within the truncated *APS3* coding sequences with EcoRV to target insertion and inactivation of the remaining *APS3* allele. Loss of the remaining *APS3* allele was confirmed by PCR with primers APS3DETF2 and APS3DETR2 with the absence of the expected 371-bp product.

Finally a wild-type copy of *VPS21*, *YPT52*, *YPT53*, or *APS3*, including 5′ and 3′ flanking sequences, was introduced into the gene deletion strains with pLUXVPS21, pLUXYPT52, pLUXYPT53, or pLUXAPS3 to produce prototrophic reconstituted strains. Isogenic gene deletion strains were produced by transforming the mutant strains with pLUX alone. Each plasmid was digested with NheI to target integration into (and reconstitute) the *URA3* loci, circumventing the well-documented positional effects of *URA3* integration (34). Correct integration and thus reconstitution of the *URA3* loci were confirmed by the presence of a 2.2-kb product following PCR with primers LUXINTDETF/R.

Strains carrying *ACT1p*-GFP-*VPS21* and either the *ACT1p*-mCherry-*YPT52* or the *ACT1p*-mCherry-*YPT53* fusion were derived from BWP17, which was sequentially transformed with NheI-linearized pKE1:GFP-VPS21 (*URA3* selection), followed by NruI-linearized pGH-mCH-YPT52 or pGH-mCH-YPT53.

Ume6p-overexpressing strains were produced by transforming *ura3*$^-$ recipient strains with pLUXACT1UME6 as described above for other pLUX-derived plasmids. The *tetO-UME6* strains were made by transforming NheI-linearized pKEtetO4 (vector control) or pKEtetO4-UME6 into strain THE1 (31).

MLT1 was genomically tagged by the approach of Gerami-Nejad et al. (29). Megaprimers MLT1GFPF and MLT1GFPR were used to amplify a GFP-*URA3* cassette from pGFP-URA3, with flanking sequences to target in-frame integration at the 3′ end of the *MLT1* ORF; *ura3*$^-$ recipient strains were transformed with this cassette. Correct integration was confirmed by PCR with primers MLT1DETF and GFPDETR2.

Stress phenotypes. *C. albicans* strains were grown overnight in YPD broth at 30°C, the cell density was adjusted to 10^7 ml^{-1} in sterile water, and serial 1:5 dilutions were performed in a 96-well plate. Cells were then applied to agar with a sterile multipronged applicator. Resistance to temperature stress was determined on YPD agar at 37 and 42°C, and osmotic stress was determined on YPD agar plus 2.5 M glycerol or 1.5 M NaCl.

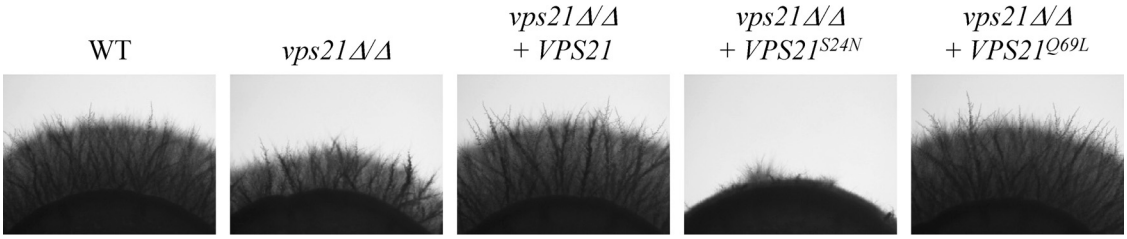

FIG 1 The active conformation of the Vps21p GTPase supports *C. albicans* hyphal growth. Inactive (*VPS21*^{S24N}) and active (*VPS21*^{Q69L}) conformational mutant alleles of *VPS21* were introduced into the *vps21*Δ/Δ mutant strain. Cell suspensions of each strain were applied as spots to M199 agar and incubated at 37°C for 4 days. Similar results were found after incubation on 10% FBS agar at 37°C (data not shown). WT, wild type.

Other stresses included YPD plus 2.5, 5, or 10 nM rapamycin; 10 mM $MnCl_2$; 12.5 or 25 μg ml^{-1} Congo red; 0.01, 0.02, or 0.05% SDS; and 250 or 500 mM $CaCl_2$.

Morphogenesis assays. Filamentous growth was assessed on M199 (pH 7.5) and 10% fetal bovine serum (FBS) agar (35). Hyphal growth was also induced in liquid M199 medium at 37°C, following inoculation of yeast at 10^6 cells ml^{-1}. In some experiments, samples of the M199 liquid cultures were taken after 0, 30, 60, 120, and 180 min and immediately fixed with formalin. Individual true hyphae were then imaged microscopically, and their lengths were determined with the CellSens Dimensions software (Olympus). Pseudohyphae (i.e., those with constrictions at cell septa) and cells that remained as yeast were not included in this analysis. *UME6*-overexpressing strains were streaked onto YPD agar plates and incubated at 30°C, and colony morphologies were compared after 24 and 48 h.

Detection of mRNA transcripts. Each strain was subcultured to either YPD at 30°C (yeast) or M199 at 37°C (hyphae) and grown for 5 h. The *TETO-UME6* mutant strains were grown overnight in YPD plus 1 μg/ml doxycycline, washed three times with sterile distilled water to remove doxycycline, and then subcultured to YPD with or without 1 μg/ml doxycycline. RNA was extracted by the hot-phenol method (36). Probes for *VPS21*, *YPT52*, *YPT53*, *ACT1*, and *HWP1* were amplified from SC5314 gDNA with primer pairs VPS21ORFF-VPS21DETR, YPT52SEQF-YPT52DETR2, YPT53ORFF-YPT53ORFR, ACT1DETF/R, and HWP1 DETF/R and labeled with the BrightStar psoralen-biotin kit (Ambion Life Technologies). Northern analysis was then conducted with the Northern Max kit (Ambion) with 30 μg of each RNA sample and detected with the BrightStar Biodetect kit in accordance with the manufacturer's recommendations.

Immunodetection of GFP fusions. Each strain was subcultured to either YPD at 30°C (yeast) or M199 medium at 37°C (hyphae) for 4 h of incubation. Cell extracts were prepared by glass bead lysis (37). Either 10 (yeast) or 40 (hyphae) μl of each lysate (supernatant fraction) was then separated by SDS-PAGE, transferred to nitrocellulose membrane, and immunoblotted with either mouse anti-GFP antibody (Santa Cruz Biotechnology catalog number 9996) at 1:200 and then a donkey anti-mouse IgG–horseradish peroxidase (HRP) conjugate (AbCam number 97030) or rabbit anti-glyceraldehyde-3-phosphate dehydrogenase (Novus Biologicals catalog number 300-327) at 1:5,000 and then a goat anti-rabbit IgG–HRP (Invitrogen catalog number 65-6120) secondary antibody. Blots were exposed by using a chemiluminescent substrate. Equivalent loading was also confirmed by staining of membranes with Ponceau red.

Fluorescence microscopy and colocalization analysis. Vacuole morphology was assessed by Cell Tracker Blue 7-amino-4-chloromethylcoumarin (CMAC; Invitrogen) staining. Yeast cells grown overnight in YPD broth were washed and resuspended at 10^7/ml in 10 mM HEPES buffer, pH 7.4, with 1% glucose. CMAC was then added at 50 μM. After 25 min at room temperature, vacuole morphology was observed with an epifluorescence microscope with a 100× objective and a UV filter set. Hyphal cells were induced in M199 medium at 37°C for 3.5 h, and CMAC was added at 100 μM. After 30 min at 37°C, cells were observed as described above, except with a 40× objective. For quantitation of colocalization, cells were grown in YPD overnight at 30°C and washed in phosphate-buffered saline and suspensions were transferred to chambered cover glass slides. Live cells were visualized on an inverted Zeiss Axiovert deconvolution microscope with a 100× objective. Images were recorded for differential interference contrast and GFP/mCherry fluorescence with Axiovision software (Zeiss). Correlation analyses of background-subtracted images were performed with the JACoP v2.1 plug-in for ImageJ (http://rsb.info.nih.gov/ij/plugins/track/jacop.html). Endocytic trafficking was assessed by pulse-labeling cells with the fluorescent dye FM4-64 (6, 38).

RESULTS

Endosomal and vacuolar GTPases are required to be in the active conformation to support *C. albicans* hyphal growth. Rab GTPases are central regulators of membrane trafficking in eukaryotes (39). Our previous work demonstrated that both PVC (Vps21p) and vacuolar (Ypt72p) Rab GTPases support *C. albicans* hyphal growth (6). We postulated that the vacuolar trafficking events required for polarized hyphal growth would depend upon activation of the Vps21p and Ypt72p GTPases. To test this, we produced mutant alleles of *VPS21* and *YPT72* encoding constitutively active and inactive conformational mutant forms of either GTPase, through manipulation of conserved amino acid residues (40–45). These alleles were then introduced into the respective *vps21*Δ/Δ and *ypt72*Δ/Δ mutant strains. Examination of hyphal growth revealed that the active mutant alleles *VPS21*^{Q69L} and *YPT72*^{Q70L} support hyphal growth, whereas the inactive *VPS21*^{S24N} and *YPT72*^{T24N} alleles do not (Fig. 1; see Fig. S1 in the supplemental material). Surprisingly, expression of the *VPS21*^{S24N} allele exacerbated the hyphal growth defect of the *vps21*Δ/Δ mutant. We considered that this may be due to the inhibition of a closely related GTPase in *trans*, a phenomenon that has been observed between GTPases that share guanine nucleotide exchange factors (41).

***C. albicans* possesses three Vps21p-like Rab GTPases.** Searches of the CGD database revealed two proteins that share significant homology with Vps21p; they are encoded by ORF19.7216 and ORF19.430 (see Table S2 in the supplemental material). Both predicted protein sequences possess the characteristic motifs of a Rab GTPase, including C-terminal (XXXCC) dual prenylation consensus sequences and the presence of five short diagnostic sequences (RabF1 to RabF5) (46). Both ORFs encode well-conserved phosphate binding (PM1 to PM3) and guanine base binding (G1 to G3) motifs. Of note, the G3 motif of ORF19.430 was incompletely conserved (encoding SSK rather than the typical SAK). *S. cerevisiae* also has two additional Vps21p-like Rab GTPases, named *YPT52* and *YPT53*, that function in vacuolar protein sorting (15, 19). There is also evidence to suggest

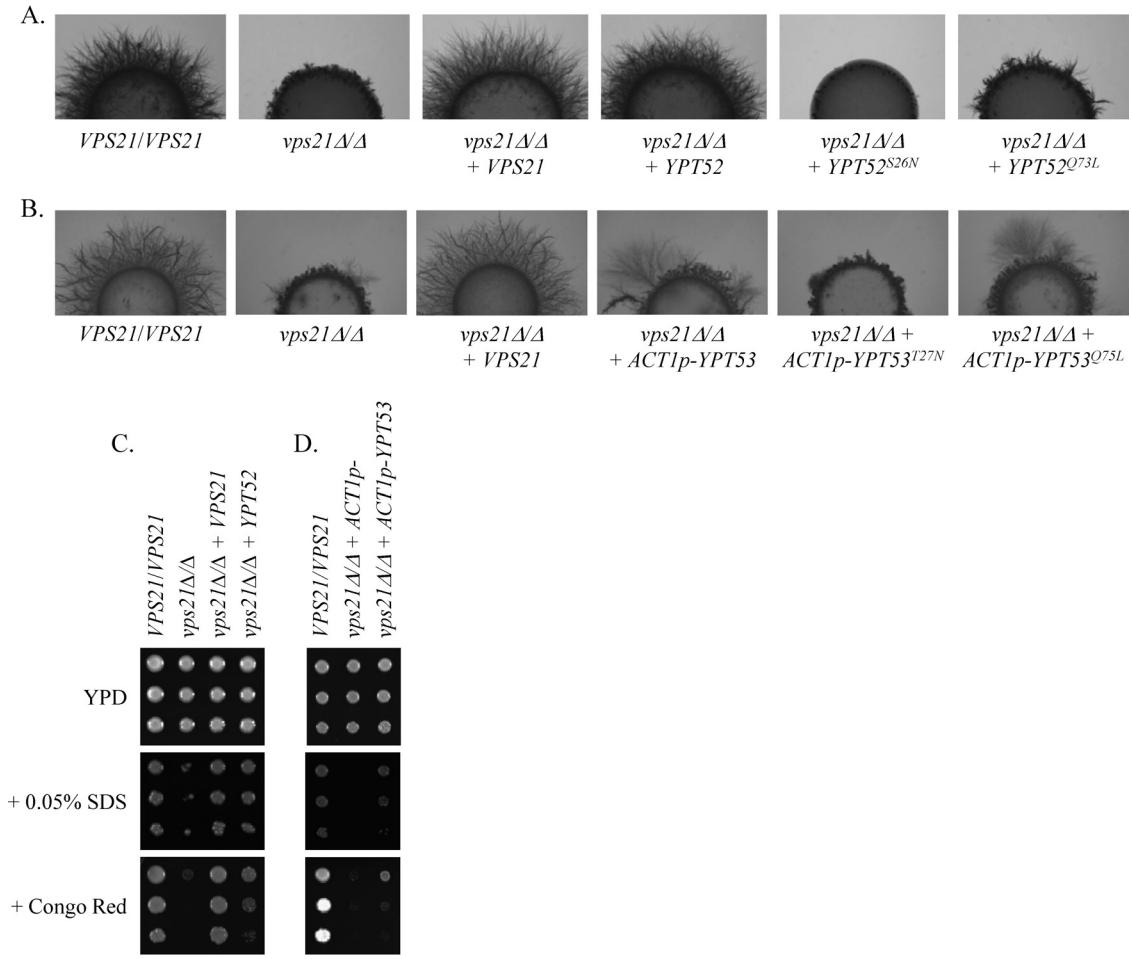

FIG 2 Ypt52p and Ypt53p can suppress *vps21*Δ/Δ mutant hyphal growth and stress defects. A wild-type allele of either *VPS21* or *YPT52* or an *ACT1p-YPT53* construct was introduced into the *vps21*Δ/Δ mutant. Similar constructs encoding putatively inactive ($YPT52^{S26N}$ and $YPT53^{T27N}$) and active ($YPT52^{Q73L}$ and $YPT53^{Q75L}$) conformational mutant alleles of either gene, were also introduced into the *vps21*Δ/Δ mutant strain (A and B only). (A and B) Cell suspensions of each strain were applied as spots to 10% FBS agar and incubated at 37°C for 4 days. Similar results were found after incubation on M199 agar at 37°C (see Fig. S3A in the supplemental material). (C and D) Cell suspensions of each strain were prepared by serial dilution, applied to YPD agar or to YPD agar supplemented with 25 μg/ml Congo red or 0.05% SDS, and incubated at 30°C for 2 days.

that there is some overlap in the GAP proteins that regulate these three GTPases (20). In keeping with the *Saccharomyces* literature, we designated the two new *C. albicans* GTPase-encoding genes *YPT52* (ORF19.7216) and *YPT53* (ORF19.430). Northern analysis detected a transcript of approximately 2.1 kb for each of the three GTPase-encoding genes (see Fig. S2 in the supplemental material) that are absent from the respective gene deletion strains (see below). The *VPS21* transcript was readily detected, suggesting that it is relatively abundant. Extended exposure times were required to detect the *YPT52* and *YPT53* transcripts, suggesting that they are present at much lower levels.

Ypt52p and Ypt53p share functional overlap with Vps21p. To determine the functional interaction between these GTPases, we increased the expression of either *YPT52* or *YPT53* in our previously constructed *vps21*Δ/Δ mutant (6). A single copy of *YPT52* was sufficient to completely rescue the hyphal growth defects of the *vps21*Δ/Δ mutant and largely rescue the previously reported sensitivity to Congo red, SDS, and rapamycin (6) (Fig. 2A and C; see Fig. S3 in the supplemental material). While *YPT53* expressed from its native promoter had little impact on the phenotypes of the *vps21*Δ/Δ mutant, when overexpressed from *ACT1p*, it partially suppressed both hyphal growth and stress defects (Fig. 2B and D; see Fig. S3). This strongly suggests that both Ypt52p and Ypt53p share significant functional overlap with Vps21p. An active conformational mutant allele, $YPT52^{Q73L}$, restored hyphal growth to the *vps21*Δ/Δ mutant (Fig. 2A) but to a lesser extent than the wild-type allele. An inactive variant, $YPT52^{S26N}$, further decreased hyphal growth, presumably because of *trans* inactivation of the endogenous wild-type *YPT52* alleles. A similar trend was observed when the equivalent conformational mutant forms of the *ACT1-YPT53* construct were introduced into the *vps21*Δ/Δ mutant strain (Fig. 2B).

Ypt52p and Ypt53p colocalize with Vps21p to a late endosomal compartment. In order to determine the cellular compartment in which these putative Rab GTPases function, we tagged the N terminus of each with GFP or mCherry. Each of the fusion proteins is functional, as determined by the suppression of *vps21*Δ/Δ mutant phenotypes (see Fig. S3). Initial analysis revealed that GFP-Ypt52p localizes to one or two subvacuolar spots (see Fig. S4), similar to the previously described

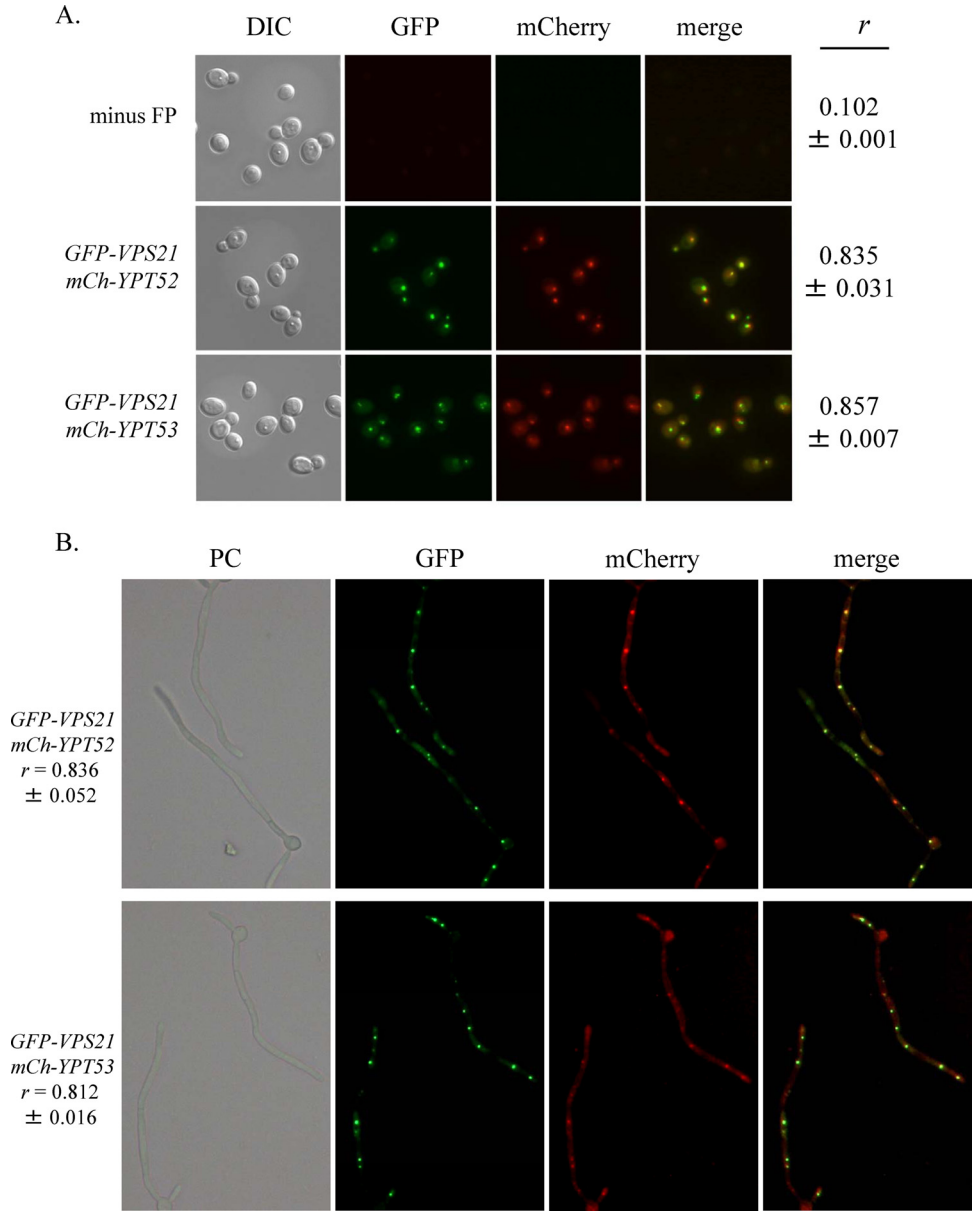

FIG 3 Ypt52p and Ypt53p colocalize with the late endosomal Rab GTPase Vps21p. GFP-*VPS21*, mCherry (*mCh*)-*YPT52*, and mCh-*YPT53* gene fusions were each expressed from *C. albicans ACT1p*. Strains harboring *ACT1p*-GFP-*VPS21* and either *ACT1p*-mCh-*YPT52* or *ACT1p*-mCh-*YPT53* were grown as either yeast cells in YPD medium at 30°C (A) or as hyphae in M199 medium at 37°C (B) and observed by phase-contrast (PC) and fluorescence microscopy with a 100× objective (A) or a 40× objective (B). Representative images are shown with Pearson's correlation coefficient (*r*) values expressed as means ± standard deviations ($n = 30$ to 50 cells). DIC, differential interference contrast.

GFP-Vps21p fusion (6). However, GFP-Ypt53p was not detectable when transcription was dependent upon the native *YPT53* 5′ and 3′ UTRs.

We next asked if Ypt52p or Ypt53p functions in the same late endosomal compartment as Vps21p. In order to enhance expression, we placed the mCherry-*YPT52* and mCherry-*YPT53* fusions under the transcriptional control of *C. albicans ACT1p*. Either fusion construct was then introduced into a strain overexpressing GFP-Vps21p (also from *ACT1p*). The cellular distribution of the GFP-Vps21p and mCh-Ypt52p fusions was the same when they were expressed from either the native promoter or *ACT1p* (Fig. 3A; see Fig. S4) (6). This revealed that much of mCh-Ypt52p and mCh-Ypt53p colocalized with GFP-Vps21p in both the yeast and hyphal forms (Fig. 3), suggesting that all three GTPases function in the same endosomal compartment(s).

Loss of *VPS21* and *YPT52* causes synthetic defects in vacuolar trafficking. To determine the functions of *YPT52* and *YPT53*, we constructed *ypt52*Δ/Δ and *ypt53*Δ/Δ, as well as *vps21*Δ/Δ *ypt52*Δ/Δ, *vps21*Δ/Δ *ypt53*Δ/Δ, and *ypt52*Δ/Δ *ypt53*Δ/Δ, gene deletion strains. For each single and double mutant, reconstituted strains were produced through the reintroduction of wild-type alleles of the deleted gene(s). We also attempted to construct a *vps21*Δ/Δ *ypt52*Δ/Δ *ypt53*Δ/Δ triple mutant. While we were able to readily delete one copy of *YPT53* from the *vps21*Δ/Δ *ypt52*Δ/Δ

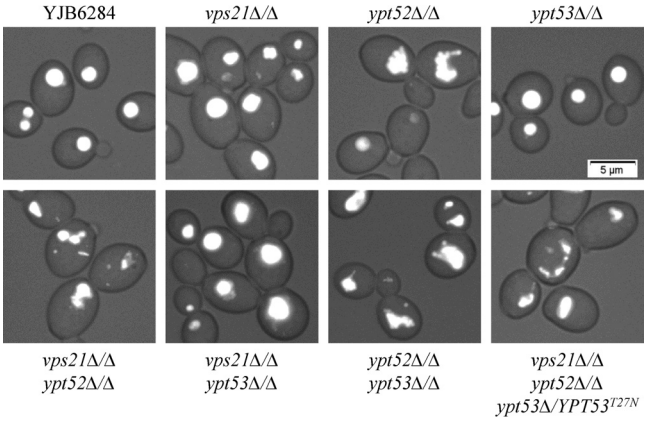

FIG 4 Ypt52p affects vacuole morphology in *C. albicans* yeast. Each strain was grown as yeast in YPD broth at 30°C, and vacuoles were stained with CMAC. Live cells were then observed by phase-contrast and fluorescence microscopy. Merged images are shown.

mutant strain, we were not able to delete the second copy, with all 150 transformants retaining an intact *YPT53* allele. Following placement of the remaining *YPT53* allele under the control of the *MET3* regulatable promoter (27), we found that suppression of expression with methionine and cysteine was not lethal (data not shown). Thus, to facilitate phenotypic analysis, we introduced a putatively inactive *YPT53*^{T27N} allele into the *vps21*Δ/Δ *ypt52*Δ/Δ *ypt53*Δ/*YPT53* mutant strain to suppress the function of the remaining *YPT53* allele.

We next visualized vacuolar integrity with the fluorescent dye CMAC. In the yeast form, the *vps21*Δ/Δ mutant strain has apparently normal spherical vacuoles while the *ypt52*Δ/Δ mutant strain has misshapen and partially fragmented vacuoles (Fig. 4; see Fig. S5 in the supplemental material). The *vps21*Δ/Δ *ypt52*Δ/Δ double and triple mutants have more severe defects, with a heterogeneous assortment of small compartments labeled with CMAC. However, loss of *YPT53* has a negligible impact on vacuolar morphology in the yeast form. These data suggest that it is principally the Vps21p and Ypt52p GTPases that contribute to vacuolar biogenesis.

Endocytic trafficking from the plasma membrane to the vacuole was assessed with the lipophilic dye FM4-64 (Fig. 5). This confirmed that the *vps21*Δ/Δ mutant is deficient in endocytosis (3, 6), with much of the dye found diffusely in the cytoplasm. This defect was exacerbated in the *vps21*Δ/Δ *ypt52*Δ/Δ double mutant, while *YPT53* again had little effect. Finally, Golgi-to-vacuole trafficking was assessed with an Mlt1-GFP fusion protein that localizes to the vacuolar membrane (Fig. 5) (47). Mlt1-GFP localization was normal in each of the single mutants, as well as the *vps21*Δ/Δ *ypt53*Δ/Δ and *ypt52*Δ/Δ *ypt53*Δ/Δ double mutants. However, significant Mlt1-GFP mislocalization occurred in the *vps21*Δ/Δ *ypt52*Δ/Δ and triple GTPase mutants, with much of the GFP detected diffusely or as punctuate spots throughout the cytoplasm. Collectively, these data underscore the redundant roles played by Vps21p and Ypt52p in facilitating endosomal trafficking to the *C. albicans* vacuole. Notably, some FM4-64 and Mlt1-GFP reached the vacuole in even the *vps21*Δ/Δ *ypt52*Δ/Δ and *vps21*Δ/Δ *ypt52*Δ/Δ *ypt53*Δ/*YPT53*^{T27N} mutants, to reveal a surprisingly large and structurally intact vacuolar compartment under these assay conditions.

Loss of *VPS21* and *YPT52* causes synthetic stress phenotypes. Severe defects in vacuolar trafficking can cause substantial reductions in *C. albicans* growth (6, 7). However, loss of either GTPase alone does not cause any substantial growth defect in YPD broth (pH 5.7) at 30 or 37°C (see Fig. S6A and B; data not shown). The *vps21*Δ/Δ *ypt52*Δ/Δ and triple mutants have a slightly reduced growth rate at either temperature (see Fig. S6B). Yeast mutants deficient in vacuolar acidification are unable to grow at neutral pH (48, 49); therefore, we also compared the growth of our mutants in YPD medium at pH 7 (see Fig. S6D, E, and F). Under these conditions, the slight growth deficiencies of the *vps21*Δ/Δ *ypt52*Δ/Δ and triple mutants were exacerbated and the *vps21*Δ/Δ *ypt53*Δ/Δ and *ypt52*Δ/Δ *ypt53*Δ/Δ mutants also exhibited very mild growth rate reductions versus the wild-type control. Nonetheless, none of the GTPase mutants exhibit the severe growth retardation of our previously reported *vps11*Δ/Δ vacuole-deficient mutant (see Fig. S6C and F) or the severe pH-sensitive growth phenotype of a v-ATPase-deficient mutant (49). Furthermore, none of the mutants were sensitive to 10 mM $MnCl_2$ (data not shown), a phenotype associated with v-ATPase dysfunction (48, 49). These data are consistent with the FM4-64/Mlt1p trafficking analysis and indicate that significant vacuolar trafficking and function are retained in even the triple GTPase mutant.

The *vps21*Δ/Δ *ypt52*Δ/Δ mutant also has synthetic stress defects, with more severe SDS-, Congo red-, and rapamycin-sensitive growth phenotypes than the *vps21*Δ/Δ mutant strain (see Fig. S7), This further supports the idea that Ypt52p and Vps21p have a significant functional overlap. None of the mutants were sensitive to $CaCl_2$ (up to 1 M) or elevated temperatures (up to 42°C) (see Fig. S7), as has been reported for the equivalent *S. cerevisiae* mutants (15, 21).

Loss of *VPS21* and *YPT52* causes synthetic hyphal growth defects. Hyphal growth was examined with 10% FBS or M199 medium on a solid agar substrate or in liquid cultures (Fig. 6A and 7). We also artificially induced hyphal growth by overexpressing the transcription factor Ume6p (see Fig. S9), which results in constitutive hyphal growth under all conditions (50). This enabled us to compare hyphal growth on YPD agar (pH 5.7), where differences in growth rate are minimal. As expected, the *vps21*Δ/Δ mutant has reduced hyphal growth versus that of the wild type (3, 6). Comparison of hyphal lengths at various time points following hyphal induction revealed that the *vps21*Δ/Δ mutant cells were delayed in germ tube emergence and had a reduced hyphal elongation rate compared to that of the control strain (see Fig. S8A). Loss of *YPT52* or *YPT53* alone or in combination has little impact on hyphal growth. However, the *vps21*Δ/Δ *ypt52*Δ/Δ double mutant has profound defects in hyphal growth, forming only very short hyphae. Interestingly, reintroduction of *VPS21* restored normal hyphal growth to the *vps21*Δ/Δ *ypt52*Δ/Δ mutant, while *YPT52* did not. This is explained by the fact that *YPT52* becomes haploinsufficient in the absence of *VPS21*, since a *vps21*Δ/Δ *ypt52*Δ/*YPT52* strain is similarly deficient in hyphal growth (Fig. 6C). Thus, the Vps21p endosomal GTPase appears to be sufficient to support normal *C. albicans* hyphal growth; however, Ypt52p plays an important secondary role in the absence of Vps21p. The role of Ypt53p in hyphal growth is much less significant but also more complex. The triple mutant was even more severely affected in hyphal growth than the *vps21*Δ/Δ *ypt52*Δ/Δ double mutant (Fig. 6B). This indicates a minor but positive role for Ypt53p in hyphal growth and is consistent with the previous observation

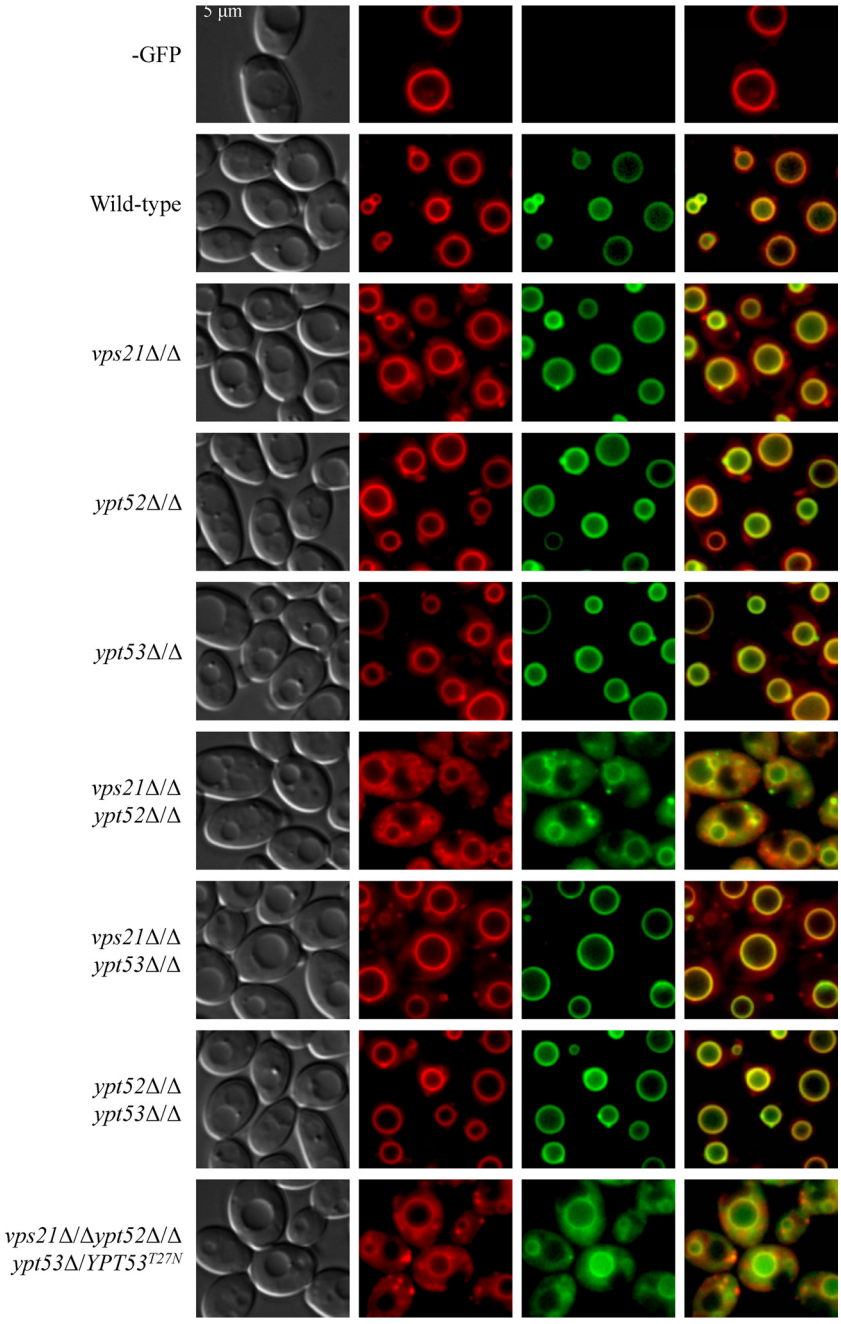

FIG 5 Vps21p and Ypt52p facilitate endocytic and biosynthetic trafficking to the *C. albicans* vacuole. The vacuolar membrane protein Mlt1p was tagged with GFP in each mutant and a wild-type control strain to evaluate biosynthetic trafficking from the Golgi compartment to the vacuole. Each strain was then pulse-chase labeled with FM4-64 to simultaneously assess trafficking from the plasma membrane via endocytosis. Cells were observed by fluorescence microscopy to determine FM4-64 (center left panels) and Mlt1-GFP (center right panels) distribution and by Nomarski optics (far left panels). Merged FM4-64-GFP images are also shown (far right panels).

that an *ACT1p-YPT53* expression construct can suppress the hyphal growth defects of the *vps21*Δ/Δ mutant. This was contradicted by the fact that the *vps21*Δ/Δ *ypt53*Δ/Δ mutant strain reproducibly formed longer hyphae than the *vps21*Δ/Δ mutant on M199 and 10% FBS agar (compare images labeled with * and also ** images in Fig. 6A). Conversely, no measureable differences in the hyphal lengths of the *vps21*Δ/Δ and *vps21*Δ/Δ *ypt53*Δ/Δ mutants were detected in liquid M199 medium (see Fig. S8A), suggesting that Ypt53p has no significant role under these conditions.

Vacuole morphology was investigated in hyphal cells by CMAC staining. Large tubular vacuoles were observed in the subapical regions of wild-type *C. albicans* hyphae (Fig. 7). However, the vacuoles in the *vps21*Δ/Δ mutant hyphae were shorter and more spherical, resembling those typically found in the yeast form. This was especially the case in the short *vps21*Δ/Δ *ypt52*Δ/Δ mutant hyphae, while the *vps21*Δ/Δ *ypt52*Δ/Δ *ypt53*Δ/*YPT53*^{T27N} triple mutant had very small round vacuoles.

Northern analysis revealed that the transcripts of all three

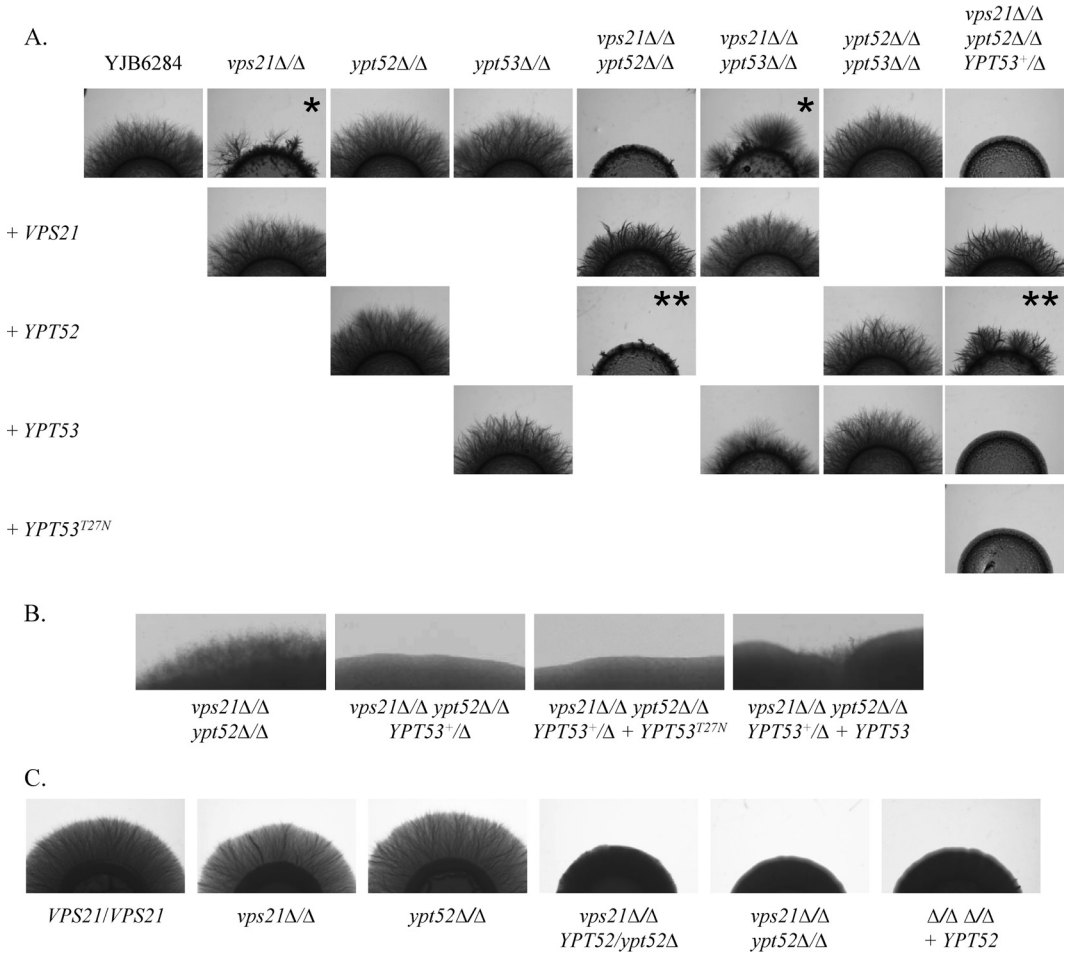

FIG 6 Loss of both Vps21p and Ypt52p causes synthetic defects in *C. albicans* hyphal growth. (A) Cell suspensions of each strain were applied as spots to 10% FBS agar and incubated at 37°C for 4 days. Similar results were found after incubation on M199 agar at 37°C (data not shown). (B) Selected strains are shown at higher magnification after 7 days of incubation on FBS agar at 37°C. (C) Cell suspensions of each strain were applied as spots to M199 agar and incubated at 37°C for 5 days. Similar results were found after incubation on FBS agar at 37°C (data not shown). Please see the text for an explanation of * and **.

GTPase-encoding genes are increased under hyphal growth conditions (see Fig. S10A). Interestingly, overexpression of the Ume6p transcription factor is sufficient to enhance the transcription of all three GTPase genes (see Fig. S10B). Finally, we compared the relative expression levels of the three GTPases in yeast and hyphal growth conditions with the GFP-tagged fusions (see Fig. S8B). In both yeast and hyphal extracts, GFP-Vps21p is the most abundant, GFP-Ypt52p is second, and GFP-Ypt53p expression is below the limit of detection. GFP-Ypt53p was also undetectable under stress conditions (0.5 M $CaCl_2$, 1.5 M NaCl, or 1.5 M sorbitol; data not shown), consistent with its largely inconsequential role in each of the phenotypes we tested.

Disruption of AP-3-mediated trafficking exacerbates the stress and hyphal growth defects of endosomal trafficking mutants. We previously demonstrated that loss of both Vps21p- and Aps3p-dependent trafficking resulted in synthetic stress phenotypes, as well as hyphal growth defects, but was not sufficient to cause significant disruption of vacuolar integrity in *C. albicans* yeast (3). We speculated that in the yeast form, Ypt52p-dependent trafficking was sufficient to maintain a morphologically intact vacuole but insufficient to support the vacuolar trafficking required for hyphal growth. To test this, we attempted to construct a *vps21*Δ/Δ *ypt52*Δ/Δ*aps3*Δ/Δ triple mutant. As was the case in constructing the triple GTPase mutant, we were able to delete the first copy of *APS3* in the *vps21*Δ/Δ *ypt52*Δ/Δ mutant background, but the second allele was problematic. We were only able to ablate the second *APS3* allele by insertional inactivation, to yield a *vps21*Δ/Δ *ypt52*Δ/Δ*aps3*Δ/− triple mutant. Unfortunately, this strategy precluded the construction of strains reconstituted with the respective wild-type alleles.

Curiously, the *vps21*Δ/Δ *ypt52*Δ/Δ*aps3*Δ/− mutant had an enlarged vacuole in the yeast form compared to the wild-type strains (Fig. 8, top panels), indicating that loss of AP-3-mediated trafficking somehow increases vacuole size in the endosome-deficient *vps21*Δ/Δ *ypt52*Δ/Δ mutant. Despite this, the *vps21*Δ/Δ *ypt52*Δ/Δ*aps3*Δ/− mutant exhibited more severe hyphal growth defects than either the *vps21*Δ/Δ *ypt52*Δ/Δ or the *vps21*Δ/Δ*aps3*Δ/Δ double mutant (Fig. 8, middle and bottom panels) and was unable to form extensively vacuolated hyphal cells. The *vps21*Δ/Δ *ypt52*Δ/Δ*aps3*Δ/− mutant also has more severe growth and stress phenotypes than either the *vps21*Δ/Δ *ypt52*Δ/Δ or the *vps21*Δ/Δ*aps3*Δ/Δ mutant (see Fig. S6C and F and S7 in the supplemental material)

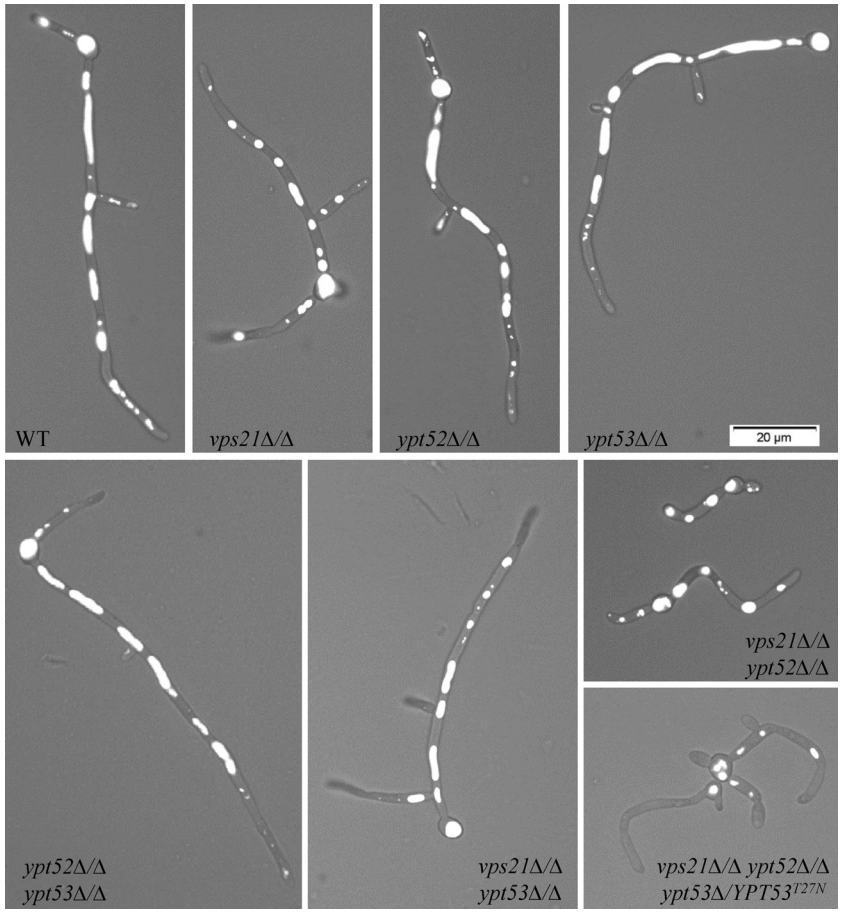

FIG 7 Loss of both Vps21p and Ypt52p causes profound defects in vacuole formation during *C. albicans* hyphal growth. Each strain was induced to form hyphae for 3.5 h in M199 medium, and vacuoles were stained with CMAC. Live cells were then observed by phase-contrast and fluorescence microscopy. Merged images are shown.

(3), indicating severe loss of vacuolar function comparable to that of the *vps11*Δ/Δ mutant strain.

Finally, our studies suggest that both Ypt52p- and Aps3p-dependent pathways play roles secondary to Vps21p-mediated trafficking, with respect to supporting *C. albicans* hyphal growth. While neither the *ypt52*Δ/Δ nor the *aps3*Δ/Δ mutant exhibits any hyphal growth defect, as anticipated, the *ypt52*Δ/Δ*aps3*Δ/Δ double mutant has a minor defect in hyphal growth (see Fig. S11). These data confirm that Ypt52p and Aps3p define distinct pathways that play important secondary roles in supporting the vacuolar trafficking required for *C. albicans* hyphal growth.

DISCUSSION

Defining the precise vacuolar trafficking mechanisms that support fungal colonization and invasion of mammalian tissue will facilitate the development of effective therapeutic strategies that target this organelle. Our previous studies revealed that the PVC Rab GTPase Vps21p makes an important contribution to *C. albicans* hyphal growth and pathogenicity (3, 6). In this study, we identified two related GTPases, Ypt52p and Ypt53p, that colocalize and show a significant functional overlap with Vps21p.

Previous studies have determined that *S. cerevisiae* also possesses three Vps21p-like GTPases (15, 19, 21, 51, 52), and clear similarities between the functions of these genes in either species were observed. First, *C. albicans* Vps21p and Ypt52p both function in endocytic, as well as biosynthetic, trafficking routes to the vacuole, as was previously demonstrated for *S. cerevisiae* (15, 19, 21). Second, loss of both *VPS21* and *YPT52* causes strong synthetic defects in vacuolar trafficking and stress tolerance in either species (15, 21). Third, despite a significant functional overlap, the three GTPases make unequal contributions to vacuolar trafficking and apparently fungal physiology as a whole. In both species, Vps21p is the most important of the three GTPases, with Ypt52p playing a secondary role and Ypt53p the least significant (15). In *C. albicans*, this correlated with the expression levels of each protein. That overexpression from *ACT1p* suppressed *vps21*Δ/Δ phenotypes indicates that *YPT53* does encode a functional protein. However, we were unable to detect expression of the GFP-Ypt53p fusion protein when transcription is dependent upon the native *YPT53* 5′ and 3′ UTRs. In *S. cerevisiae*, transcription of *YPT53* is induced by high Ca^{2+} levels (21). However, this was not the case in *C. albicans* (data not shown). Thus, the very low expression levels of Ypt53p may explain its largely inconsequential role in *C. albicans* physiology. The incomplete conservation of the G3 guanine base binding motif in Ypt53p may also decrease the protein's activity and/or stability.

Our *C. albicans* endosomal GTPase mutants did not yield entirely the same phenotypes described for the equivalent *S. cerevi-*

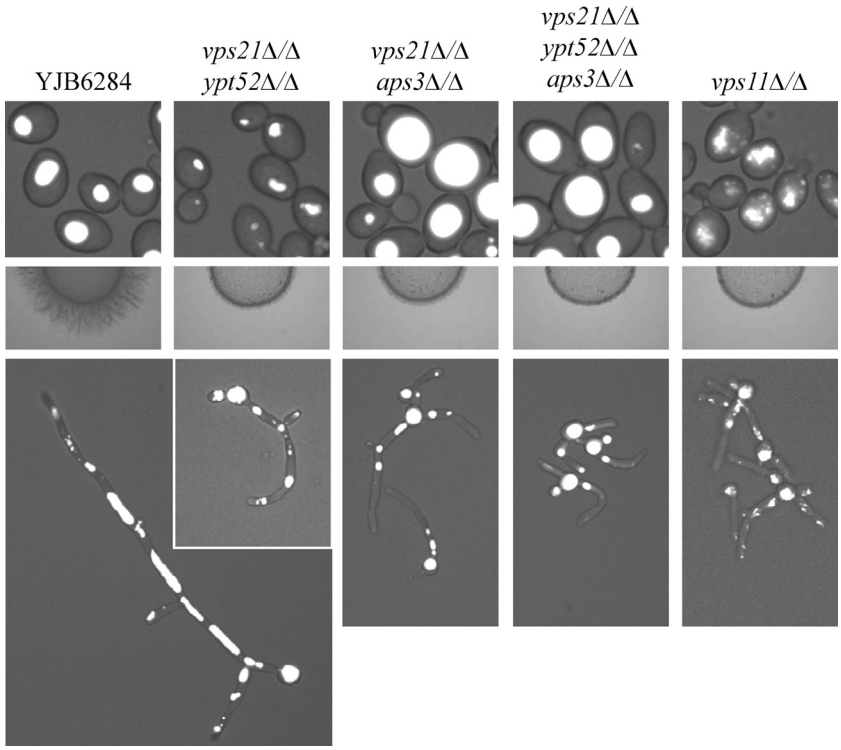

FIG 8 Loss of AP-3 trafficking dramatically increases vacuolar size in the endosome-deficient *vps21*Δ/Δ *ypt52*Δ/Δ mutant yeast but exacerbates the hyphal growth defects. Vacuole morphology was determined by CMAC staining of yeast cells grown in YPD at 30°C (top panels) or hyphal cells grown in M199 medium at 37°C (bottom panels). Hyphal growth on 10% FBS agar was also compared (center panels).

siae mutants. None of the *C. albicans* mutants exhibited the temperature- or calcium-sensitive growth phenotypes that have been reported for *S. cerevisiae* mutants (15, 21). It is unclear if this is due to species-specific functions of the endosomal Rab GTPases, or if these differences indicate divergence in the biological function of the PVC and vacuole between these fungi.

Loss of all three PVC GTPases in the *vps21*Δ/Δ *ypt52*Δ/Δ *ypt53*Δ/*YPT53*^{T27N} triple mutant resulted in synthetic phenotypes, including disrupted vacuolar trafficking, a reduced growth rate, and severely retarded hyphal formation. However, these defects were not as severe as those of the previously described *vps11*Δ/Δ or *vps21*Δ/Δ *ypt72*Δ/Δ *C. albicans* mutants (6, 7, 9). Vacuoles in the triple GTPase mutant remained intact, and trafficking of FM4-64 and Mlt1-GFP to the vacuole was not completely blocked. This indicates that other, presumably nonendosomal, vacuolar trafficking pathways remain intact in the *vps21*Δ/Δ *ypt52*Δ/Δ *ypt53*Δ/*YPT53*^{T27N} mutant that are able to sustain some level of vacuolar integrity and function. We considered that the nonendosomal Aps3p-dependent route was likely to account for the vestigial vacuolar function in the triple GTPase mutant. Surprisingly, however, the *vps21*Δ/Δ *ypt52*Δ/Δ*aps3*Δ/− triple mutant had grossly enlarged vacuoles versus those of the *vps21*Δ/Δ *ypt52*Δ/Δ and wild-type controls. Despite this, normal vacuolar function was not restored, since the *vps21*Δ/Δ *ypt52*Δ/Δ*aps3*Δ/− strain had growth, stress, and hyphal formation defects even more severe than those of the triple GTPase mutant. The pathways responsible for sustaining vacuolar structural integrity in the *vps21*Δ/Δ *ypt52*Δ/Δ*aps3*Δ/− triple mutant remain unknown. It is possible that this role could be fulfilled by Ypt53p-dependent vacuolar trafficking; however, this seems unlikely to be sufficient because of the very low expression and activity of this GTPase. Unfortunately, because of the technical limitations of using a recyclable *URA3* gene deletion cassette, we were unable to construct a *vps21*Δ/Δ *ypt52*Δ/Δ *ypt53*Δ/Δ*aps3*Δ/Δ quadruple mutant to test this.

Of the three single PVC GTPase mutants, only the *ypt52*Δ/Δ mutant exhibited obvious morphological defects of the vacuole when grown in the yeast form, whereas only the *vps21*Δ/Δ mutant had vacuolar morphology defects under hypha-inducing conditions. This could indicate that these GTPases make differential contributions to vacuolar biogenesis in the yeast and hyphal forms of *C. albicans*. Consistent with the other phenotypes, Vps21p has the greatest effect on *C. albicans* hyphal growth, with Ypt52p playing a secondary role and Ypt53p having little impact. Each of the PVC and vacuolar GTPases that we have so far examined seems to be required to be in their active conformation in order to support the polarized hyphal growth of *C. albicans*. In addition, transcription of *VPS21*, *YPT52*, and *YPT53* is elevated under hyphal growth conditions. This is not surprising, given the dynamic changes in vacuolar morphology that occur during germ tube emergence, which necessitates the rapid redistribution of cellular membrane to facilitate subapical vacuolation (12, 53). It seems likely that increased transcription of the three PVC GTPases is an indication of how vacuolar trafficking is adjusted to support hyphal growth and represents an important mechanism underlying hyphal development. Overexpression of the Ume6p transcription factor is sufficient to sustain not only polarized hyphal growth (50) but also formation of the highly vacuolated subapical hyphal cells (3)

and elevate the transcription of *VPS21*, *YPT52*, and *YPT53*. This provides further evidence that Ume6p-dependent transcriptional responses coordinately regulate cell polarization for apical growth, with subapical vacuolation.

In *S. cerevisiae*, vacuolar acidification was severely impaired by the loss of *VPS21* alone or in combination with *YPT52* (15). *C. albicans* v-ATPase-deficient mutants are defective in hyphal growth and virulence (49). Thus, we considered that the hyphal defects of our PVC-trafficking mutants could be a consequence of disrupted v-ATPase activity or transport. Unexpectedly, none of our PVC GTPase mutants exhibited the calcium-, manganese-, or pH-sensitive growth phenotypes of v-ATPase-deficient mutants, suggesting that v-ATPase activity is intact. One possible explanation is that v-ATPase trafficking is incompletely blocked, as was the case for the Mlt1p vacuolar membrane protein. A second is that there are two distinct v-ATPase complexes defined by two "a" subunits, Vph1p (vacuolar) and Stv1p (Golgi compartment) (54). Recent data suggest that loss of both Golgi compartment and vacuolar complexes may be necessary to severely impact *C. albicans* hyphal growth (55). Interestingly, the vacuolar membrane protein Mlt1p has also been implicated in the capacity of *C. albicans* to cause disease (47). The results of this and our previous study (3) demonstrate that this protein can reach the vacuole via Vps21p-, Ypt52p-, or Aps3p-dependent trafficking routes. Finally, the *vps21*Δ/Δ mutant's rapamycin sensitivity is suggestive of deficiencies in TOR kinase signaling (6, 52). It will be interesting to determine if the stress or hyphal defects of the *C. albicans vps21*Δ/Δ and *vps21*Δ/Δ *ypt52*Δ/Δ mutants are related to deficiencies in TOR kinase signaling, or are purely a secondary consequence of vacuolar dysfunction.

Current efforts in our lab are geared toward the identification of small molecules that disrupt the integrity of the fungal vacuole and/or associated trafficking mechanisms. Continued exploration of the vacuole-associated mechanisms or pathways that support fungal pathogenesis, and in the case of *C. albicans*, virulence-associated hyphal growth, will help facilitate efforts to exploit this organelle as a target for antifungal therapy.

ACKNOWLEDGMENTS

Research reported in this publication was supported by the National Institute of Allergy and Infectious Diseases of the National Institutes of Health under awards R21AI097664 and R56AI099080. The content is solely our responsibility and does not necessarily represent the official views of the National Institutes of Health.

We thank Aaron Mitchell (Carnegie Mellon University) and William Fonzi (Georgetown University) for strains and plasmid constructs. We also thank H. Nakayama and M. Arisawa (Nippon Roche) for providing the materials required for the *C. albicans* tetracycline-regulatable system. Thanks also to the LSUHSC Gene Therapy Program's Morphology and Imaging Core for assistance with imaging.

REFERENCES

1. **Hu G, Hacham M, Waterman SR, Panepinto J, Shin S, Liu X, Gibbons J, Valyi-Nagy T, Obara K, Jaffe HA, Ohsumi Y, Williamson PR.** 2008. PI3K signaling of autophagy is required for starvation tolerance and virulence of *Cryptococcus neoformans*. J. Clin. Invest. **118:**1186–1197.
2. **Liu X, Hu G, Panepinto J, Williamson PR.** 2006. Role of a *VPS41* homologue in starvation response, intracellular survival and virulence of *Cryptococcus neoformans*. Mol. Microbiol. **61:**1132–1146.
3. **Palmer GE.** 2010. Endosomal and AP-3-dependent vacuolar trafficking routes make additive contributions to *Candida albicans* hyphal growth and pathogenesis. Eukaryot. Cell **9:**1755–1765.
4. **Hilty J, Smulian AG, Newman SL.** 2008. The *Histoplasma capsulatum* vacuolar ATPase is required for iron homeostasis, intracellular replication in macrophages and virulence in a murine model of histoplasmosis. Mol. Microbiol. **70:**127–139.
5. **Roetzer A, Gratz N, Kovarik P, Schuller C.** 2010. Autophagy supports *Candida glabrata* survival during phagocytosis. Cell. Microbiol. **12:**199–216.
6. **Johnston DA, Eberle KE, Sturtevant JE, Palmer GE.** 2009. Role for endosomal and vacuolar GTPases in *Candida albicans* pathogenesis. Infect. Immun. **77:**2343–2355.
7. **Palmer GE, Kelly MN, Sturtevant JE.** 2005. The *Candida albicans* vacuole is required for differentiation and efficient macrophage killing. Eukaryot. Cell **4:**1677–1686.
8. **Erickson T, Liu L, Gueyikian A, Zhu X, Gibbons J, Williamson PR.** 2001. Multiple virulence factors of *Cryptococcus neoformans* are dependent on *VPH1*. Mol. Microbiol. **42:**1121–1131.
9. **Palmer GE, Cashmore A, Sturtevant J.** 2003. *Candida albicans VPS11* is required for vacuole biogenesis and germ tube formation. Eukaryot. Cell **2:**411–421.
10. **Lo HJ, Kohler JR, DiDomenico B, Loebenberg D, Cacciapuoti A, Fink GR.** 1997. Nonfilamentous *C. albicans* mutants are avirulent. Cell **90:**939–949.
11. **Saville SP, Lazzell AL, Monteagudo C, Lopez-Ribot JL.** 2003. Engineered control of cell morphology in vivo reveals distinct roles for yeast and filamentous forms of *Candida albicans* during infection. Eukaryot. Cell **2:**1053–1060.
12. **Gow NA, Gooday GW.** 1982. Vacuolation, branch production and linear growth of germ tubes in *Candida albicans*. J. Gen. Microbiol. **128:**2195–2198.
13. **Conibear E, Stevens TH.** 1995. Vacuolar biogenesis in yeast: sorting out the sorting proteins. Cell **83:**513–516.
14. **Horazdovsky BF, Busch GR, Emr SD.** 1994. *VPS21* encodes a rab5-like GTP binding protein that is required for the sorting of yeast vacuolar proteins. EMBO J. **13:**1297–1309.
15. **Singer-Krüger B, Stenmark H, Dusterhoft A, Philippsen P, Yoo JS, Gallwitz D, Zerial M.** 1994. Role of three rab5-like GTPases, Ypt51p, Ypt52p, and Ypt53p, in the endocytic and vacuolar protein sorting pathways of yeast. J. Cell Biol. **125:**283–298.
16. **Gerrard SR, Bryant NJ, Stevens TH.** 2000. *VPS21* controls entry of endocytosed and biosynthetic proteins into the yeast prevacuolar compartment. Mol. Biol. Cell **11:**613–626.
17. **Cowles CR, Odorizzi G, Payne GS, Emr SD.** 1997. The AP-3 adaptor complex is essential for cargo-selective transport to the yeast vacuole. Cell **91:**109–118.
18. **Stepp JD, Huang K, Lemmon SK.** 1997. The yeast adaptor protein complex, AP-3, is essential for the efficient delivery of alkaline phosphatase by the alternate pathway to the vacuole. J. Cell Biol. **139:**1761–1774.
19. **Cabrera M, Arlt H, Epp N, Lachmann J, Griffith J, Perz A, Reggiori F, Ungermann C.** 2013. Functional separation of endosomal fusion factors and the class C core vacuole/endosome tethering (CORVET) complex in endosome biogenesis. J. Biol. Chem. **288:**5166–5175.
20. **Lachmann J, Barr FA, Ungermann C.** 2012. The Msb3/Gyp3 GAP controls the activity of the Rab GTPases Vps21 and Ypt7 at endosomes and vacuoles. Mol. Biol. Cell **23:**2516–2526.
21. **Nickerson DP, Russell MR, Lo SY, Chapin HC, Milnes JM, Merz AJ.** 2012. Termination of isoform-selective Vps21/Rab5 signaling at endolysosomal organelles by Msb3/Gyp3. Traffic **13:**1411–1428.
22. **Russell MR, Shideler T, Nickerson DP, West M, Odorizzi G.** 2012. Class E compartments form in response to ESCRT dysfunction in yeast due to hyperactivity of the Vps21 Rab GTPase. J. Cell Sci. **125:**5208–5220.
23. **Burke D, Dawson D, Stearns T.** 2000. Methods in yeast genetics: a Cold Spring Harbor Laboratory course manual. Cold Spring Harbor Laboratory Press, Cold Spring Harbor, NY.
24. **Wilson RB, Davis D, Mitchell AP.** 1999. Rapid hypothesis testing with *Candida albicans* through gene disruption with short homology regions. J. Bacteriol. **181:**1868–1874.
25. **Wilson RB, Davis D, Enloe BM, Mitchell AP.** 2000. A recyclable *Candida albicans URA3* cassette for PCR product-directed gene disruptions. Yeast **16:**65–70.
26. **Ramón AM, Fonzi WA.** 2003. Diverged binding specificity of Rim101p, the *Candida albicans* ortholog of PacC. Eukaryot. Cell **2:**718–728.
27. **Care RS, Trevethick J, Binley KM, Sudbery PE.** 1999. The *MET3* promoter: a new tool for *Candida albicans* molecular genetics. Mol. Microbiol. **34:**792–798.

28. **Gillum AM, Tsay EY, Kirsch DR.** 1984. Isolation of the *Candida albicans* gene for orotidine-5′-phosphate decarboxylase by complementation of *S. cerevisiae ura3* and *E. coli pyrF* mutations. Mol. Gen. Genet. **198:**179–182.
29. **Gerami-Nejad M, Berman J, Gale CA.** 2001. Cassettes for PCR-mediated construction of green, yellow, and cyan fluorescent protein fusions in *Candida albicans*. Yeast **18:**859–864.
30. **Gerami-Nejad M, Dulmage K, Berman J.** 2009. Additional cassettes for epitope and fluorescent fusion proteins in *Candida albicans*. Yeast **26:** 399–406.
31. **Nakayama H, Mio T, Nagahashi S, Kokado M, Arisawa M, Aoki Y.** 2000. Tetracycline-regulatable system to tightly control gene expression in the pathogenic fungus *Candida albicans*. Infect. Immun. **68:**6712–6719.
32. **Gietz D, St Jean A, Woods RA, Schiestl RH.** 1992. Improved method for high efficiency transformation of intact yeast cells. Nucleic Acids Res. **20:**1425.
33. **Boeke JD, LaCroute F, Fink GR.** 1984. A positive selection for mutants lacking orotidine-5′-phosphate decarboxylase activity in yeast: 5-fluoro-orotic acid resistance. Mol. Gen. Genet. **197:**345–346.
34. **Lay J, Henry LK, Clifford J, Koltin Y, Bulawa CE, Becker JM.** 1998. Altered expression of selectable marker *URA3* in gene-disrupted *Candida albicans* strains complicates interpretation of virulence studies. Infect. Immun. **66:**5301–5306.
35. **Palmer GE, Sturtevant JE.** 2004. Random mutagenesis of an essential *Candida albicans* gene. Curr. Genet. **46:**343–356.
36. **Collart MA, Oliviero S.** 2001. Preparation of yeast RNA. Curr. Protoc. Mol. Biol. **23:**13.12.1–13.12.5.
37. **Harlow E, Lane D.** 2006. Immunoprecipitation: lysing yeast cells using glass beads. CSH Protoc. **2006**(4).pii:pdb.prot4533. doi:10.1101/pdb.prot4533.
38. **Vida TA, Emr SD.** 1995. A new vital stain for visualizing vacuolar membrane dynamics and endocytosis in yeast. J. Cell Biol. **128:**779–792.
39. **Deneka M, Neeft M, van der Sluijs P.** 2003. Regulation of membrane transport by rab GTPases. Crit. Rev. Biochem. Mol. Biol. **38:**121–142.
40. **Dinneen JL, Ceresa BP.** 2004. Expression of dominant negative *rab5* in HeLa cells regulates endocytic trafficking distal from the plasma membrane. Exp. Cell Res. **294:**509–522.
41. **Feig LA.** 1999. Tools of the trade: use of dominant-inhibitory mutants of Ras-family GTPases. Nat. Cell Biol. **1:**E25–E27.
42. **Gorvel JP, Chavrier P, Zerial M, Gruenberg J.** 1991. rab5 controls early endosome fusion in vitro. Cell **64:**915–925.
43. **Méresse S, Gorvel JP, Chavrier P.** 1995. The rab7 GTPase resides on a vesicular compartment connected to lysosomes. J. Cell Sci. **108**(Pt 11): 3349–3358.
44. **Stenmark H, Parton RG, Steele-Mortimer O, Lutcke A, Gruenberg J, Zerial M.** 1994. Inhibition of rab5 GTPase activity stimulates membrane fusion in endocytosis. EMBO J. **13:**1287–1296.
45. **Vitelli R, Santillo M, Lattero D, Chiariello M, Bifulco M, Bruni CB, Bucci C.** 1997. Role of the small GTPase Rab7 in the late endocytic pathway. J. Biol. Chem. **272:**4391–4397.
46. **Pereira-Leal JB, Seabra MC.** 2000. The mammalian Rab family of small GTPases: definition of family and subfamily sequence motifs suggests a mechanism for functional specificity in the Ras superfamily. J. Mol. Biol. **301:**1077–1087.
47. **Theiss S, Kretschmar M, Nichterlein T, Hof H, Agabian N, Hacker J, Kohler GA.** 2002. Functional analysis of a vacuolar ABC transporter in wild-type *Candida albicans* reveals its involvement in virulence. Mol. Microbiol. **43:**571–584.
48. **Kane PM.** 2006. The where, when, and how of organelle acidification by the yeast vacuolar H^+-ATPase. Microbiol. Mol. Biol. Rev. **70:**177–191.
49. **Poltermann S, Nguyen M, Gunther J, Wendland J, Hartl A, Kunkel W, Zipfel PF, Eck R.** 2005. The putative vacuolar ATPase subunit Vma7p of *Candida albicans* is involved in vacuole acidification, hyphal development and virulence. Microbiology **151**(Pt 5):1645–1655.
50. **Carlisle PL, Banerjee M, Lazzell A, Monteagudo C, Lopez-Ribot JL, Kadosh D.** 2009. Expression levels of a filament-specific transcriptional regulator are sufficient to determine *Candida albicans* morphology and virulence. Proc. Natl. Acad. Sci. U. S. A. **106:**599–604.
51. **Liu Y, Nakatsukasa K, Kotera M, Kanada A, Nishimura T, Kishi T, Mimura S, Kamura T.** 2011. Non-SCF-type F-box protein Roy1/Ymr258c interacts with a Rab5-like GTPase Ypt52 and inhibits Ypt52 function. Mol. Biol. Cell **22:**1575–1584.
52. **Bridges D, Fisher K, Zolov SN, Xiong T, Inoki K, Weisman LS, Saltiel AR.** 2012. Rab5 proteins regulate activation and localization of target of rapamycin complex 1. J. Biol. Chem. **287:**20913–20921.
53. **Palmer GE.** 2011. Vacuolar trafficking and *Candida albicans* pathogenesis. Commun. Integr. Biol. **4:**240–242.
54. **Finnigan GC, Cronan GE, Park HJ, Srinivasan S, Quiocho FA, Stevens TH.** 2012. Sorting of the yeast vacuolar-type, proton-translocating ATPase enzyme complex (V-ATPase): identification of a necessary and sufficient Golgi/endosomal retention signal in Stv1p. J. Biol. Chem. **287:** 19487–19500.
55. **Raines SM, Rane HS, Bernardo SM, Binder JL, Lee SA, Parra KJ.** 2013. Deletion of vacuolar proton-translocating ATPase V(o)a isoforms clarifies the role of vacuolar pH as a determinant of virulence-associated traits in *Candida albicans*. J. Biol. Chem. **288:**6190–6201.